

Showcasing research from Professor Yohsuke Yamamoto's laboratory, Graduate School of Science, Hiroshima University, Hiroshima, Japan.

Synthesis and characterization of a pair of O-fac/O-mer 12-P-6 alkyloxaphosphates with a P-O-C-C four-membered ring

Phosphorus's various coordination numbers and bonding geometries enable its versatile roles in synthetic chemistry as well as biological systems. Our laboratory studies the synthesis and stereoisomerisation of hypervalent organophosphorus compounds. This work reports the first synthesis of a pair of O-facial and O-meridional hexacoordinate oxaphosphates from O-apical and O-equatorial β -hydroxyalkylphosphorane precursors. This was achieved by installing bulky groups on the ligand backbone. This synthesis helps us to understand the bonding characteristics and stereoselectivity of these molecules for devising applications in organic synthesis.

As featured in:



See Yohsuke Yamamoto *et al.*, *Chem. Sci.*, 2019, **10**, 3466.



ROYAL SOCIETY
OF CHEMISTRY | Celebrating
IYPT 2019

rsc.li/chemical-science

Registered charity number: 207890


 Cite this: *Chem. Sci.*, 2019, **10**, 3466

All publication charges for this article have been paid for by the Royal Society of Chemistry

Received 19th November 2018

Accepted 15th February 2019

DOI: 10.1039/c8sc05158e

rsc.li/chemical-science

Introduction

Hypervalent phosphorus compounds, closely related to the phosphoryl transfer reaction in biological systems,^{1,2} have been attractive subjects for both experimental and theoretical chemists.^{3,4} In the context of synthetic organic chemistry, penta-coordinate phosphoranes have been the centre of studies related to Wittig reactions⁵ since the first report of the penta-phenylphosphorane (Ph_5P),⁶ revealing their characteristic apicophilicity^{7–11} and facile stereomutation.^{12–15} This, subsequently, leads to the later development of geometrically constrained T-shaped phosphorus(^{III}) compounds¹⁶ for small molecule activation and catalysis,¹⁷ as well as the increasing number of applications of phosphonium as Lewis acids in Frustrated Lewis Pair (FLP) chemistry.^{18,19}

In contrast to the diverse applications derived from bond cleavage and formation processes of the phosphorane chemistry, hexacoordinate phosphates have mostly been used as chiral moieties for resolving enantiomeric species,^{20–25} and weakly coordinating anions for stabilizing highly reactive cationic species.²⁶ The stereoselective synthesis and isolation of

different diastereomers of heteroleptic systems remains a challenge, with few examples of hexacoordinate organophosphates that have been structurally confirmed to date (selected examples are shown in Chart 1a).^{1,27–30} This has been a persistent bottleneck for the understanding of bonding characteristics and the reactivity of hexacoordinate organophosphates, preventing them from finding wider applications in organic synthesis.³¹

The most general method of generating an octahedral hexacoordinate phosphate is by intramolecular nucleophilic addition to a pentacoordinate phosphorane center. With three bidentate ligands such as Martin's *ortho*-substituted aryl ligand (Chart 1b),^{32–37} both facial (*fac*-) and meridional (*mer*-) isomers may be formed theoretically. Typically, the meridional isomer is obtained because of the kinetic preference to the lower lying $\sigma_{(\text{P}-\text{O})}^*$ orbital over the $\sigma_{(\text{P}-\text{C})}^*$ orbital.²⁷ In spite of the fact that both *fac*- and *mer*-isomers of hexacoordinate silicon complexes and metal chelates^{38–40} are well documented, to the best of our knowledge, only one facial derivative of hexacoordinate phosphate has been reported, by Gates and coworkers, based on a homoleptic O/N ligand system.⁴¹ Until now, strategies for controlling the stereochemistry of heteroleptic hexacoordinate systems have not been achieved.

Herein we report the first stereo-pure isolation of a pair of O-*fac* and O-*mer* isomers of 12-P-6 oxaphosphates (Chart 1c) from the corresponding pentacoordinate O-equatorial/O-apical phosphoranes.^{32–36,42,43} This was achieved by using a modified Martin ligand^{37,44–46} with two bulky C_2F_5 groups to slow down the Berry pseudorotation (BPR) of the precursors.^{37,44,45} Both experimental and theoretical evidence on their structures and formation will be presented, which contributes to the

^aDepartment of Chemistry, Graduate School of Science, Hiroshima University, Higashi-hiroshima, 7398526, Japan. E-mail: yyama@sci.hiroshima-u.ac.jp

^bCollege of Applied Chemistry, Shenyang University of Chemical Technology, Shenyang, 110142, China

^cDepartment of Chemistry, Division of Natural and Exact Sciences, University of Guanajuato, Campus Gto, Noria Alta s/n 36050, Guanajuato, Mexico

† Electronic supplementary information (ESI) available: Synthetic and computational details, X-ray crystallographic data and NMR spectra. CCDC 1856674–1856678. For ESI and crystallographic data in CIF or other electronic format see DOI: 10.1039/c8sc05158e



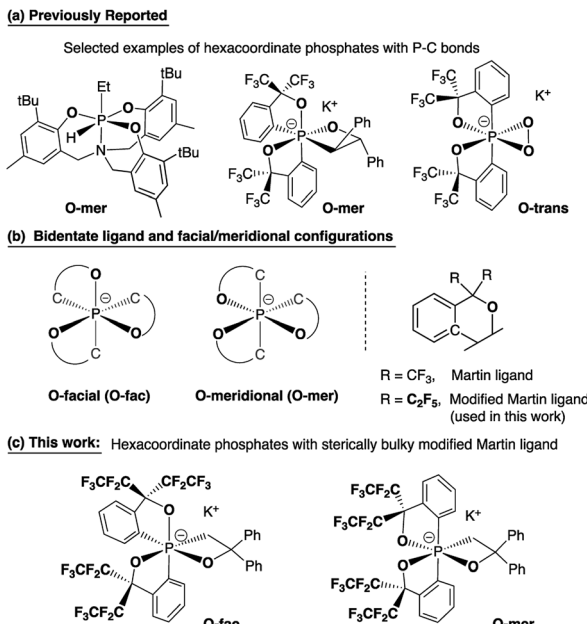


Chart 1 Bidentate ligands, O-facial/O-meridional steric configurations, and design strategies for O-fac/O-mer hexacoordinate phosphates.

formulation of a viable strategy for diastereoselective synthesis of hexacoordinate phosphates and call for further investigations into their isomerization mechanisms and reactivity.

Results and discussion

Previously, by using the pentafluoroethyl derivative of the Martin ligand to increase the steric hindrance in the BPR process, we were able to isolate both O-equatorial (**1**) and O-apical pentacoordinate methylphosphoranes (**2**).³⁷ Compound **1** is thermodynamically less stable than **2** and readily isomerizes to **2** upon heating.³⁷ Deprotonation of **1** and **2** followed by the addition of benzophenone lead to the formation of **3** and **4**, which are precursors to our target hexacoordinate phosphates (Scheme 1). X-ray crystallographic analysis of single crystals confirmed the preservation of the O-equatorial and O-apical geometries (Fig. 1 and Table S1†).⁴⁷ $^{19}\text{F}\{^1\text{H}\}$ and $^{13}\text{C}\{^1\text{H}\}$ and

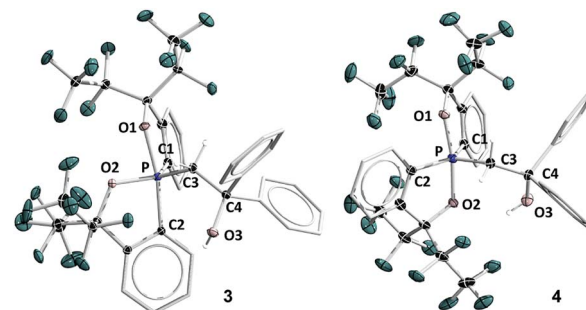
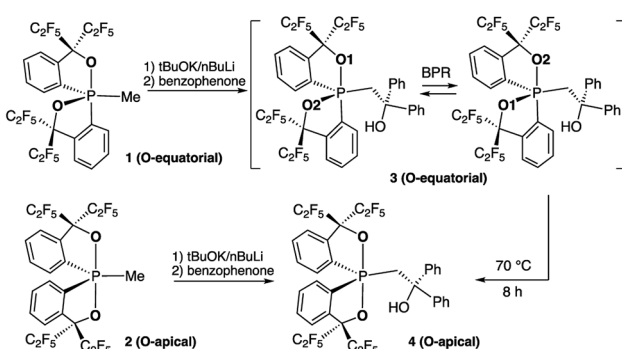


Fig. 1 ORTEP diagrams of **3** (ref. 50) and **4** showing thermal ellipsoids at the 30% probability level. Aryl carbon and hydrogen atoms are omitted for clarity. Selected distances (Å) for **4**: P1–O1, 1.753(2); P1–O2, 1.790(2); P1–C1, 1.831(3); P1–C2, 1.830(3); P1–C3, 1.838(3); C3–C4, 1.561(4); O3–C4, 1.422(4). CCDC: 1856674 for **3**; 1856675 for **4**.

^1H NMR experiments of **3** in chloroform carried out at room temperature showed equivalent signals of the ligand, indicating an equilibrium between the pair of one-step BPR isomers of **3** in solution.⁴⁸ In contrast, no dynamic behaviours were detected from the NMR spectra of **4**, suggesting a single isomer in solution at room temperature (see the spectra in the ESI†). The $^{31}\text{P}\{^1\text{H}\}$ NMR spectra of **3** and **4** showed a singlet at -2.1 ppm and -15.7 ppm respectively, consistent with pentacoordinate phosphorus environments. At elevated temperatures in benzene, the O-equatorial isomer **3** slowly converts to the O-apical isomer **4** quantitatively (Scheme 1), consistent with previous observations.^{11,37,48} The calculated energy difference between **3** and **4** is 6.8 kcal mol $^{-1}$ ((SMD:thf) ω -B97XD/def2-tzvpp// ω -B97XD/def2-svp),⁴⁹ in agreement with the experimental observations.

Deprotonation of pentacoordinate precursors **3** and **4** in THF by KH at 0 °C followed by intramolecular nucleophilic attack of the oxide lead to isolation of hexacoordinate phosphates. The reactions were monitored by $^{31}\text{P}\{^1\text{H}\}$ NMR spectroscopy. In the reaction of the O-equatorial phosphorane **3**, the reaction completes within 30 minutes to afford a new compound **5B** in 85% isolated yield. The ^{31}P NMR spectrum of **5B** in CD_3CN at room temperature showed a singlet at -107.8 ppm, characteristic of a hexacoordinate phosphate (ESI†). Furthermore, in the ^1H NMR spectrum, the originally equivalent hydrogen atoms (by BPR) on the methylene protons (CH_2) observed in **3** ($\delta = 3.84$ (d, $^2J_{\text{HP}} = 15.6$ Hz, 2H) at 25 °C) gave rise to two sets of distinct proton signals at 4.19 ppm (dd, $^2J_{\text{HP}} = 30$ Hz, $^2J_{\text{HH}} = 12$ Hz, 1H) and 3.21 ppm (dd, $^2J_{\text{HP}} = 12$ Hz, $^2J_{\text{HH}} = 12$ Hz, 1H), consistent with a restricted P–C3 bond in a four-membered ring. Also, the ^{19}F NMR spectrum showed four distinguishable quartets for $-\text{CF}_3$ groups. These observations suggest a hexacoordinate structure of **5B** in CD_3CN at room temperature.

The structure of **5B** was confirmed from single-crystal X-ray crystallographic analysis, which revealed a hexacoordinate O-facial geometry. The solid-state structure of **5B** (Fig. 2 and Table S1†) shows a facial coordination of the potassium to all the oxygen atoms. This cation coordination can be prevented by addition of 18-crown-6 to the reaction mixture, which suggests that the facial coordination of potassium cation is not a crucial



Scheme 1 Synthesis of pentacoordinate alkylxaphosphoranes **3** and **4** with a $-\text{CH}_2\text{CPh}_2\text{OH}$ group.

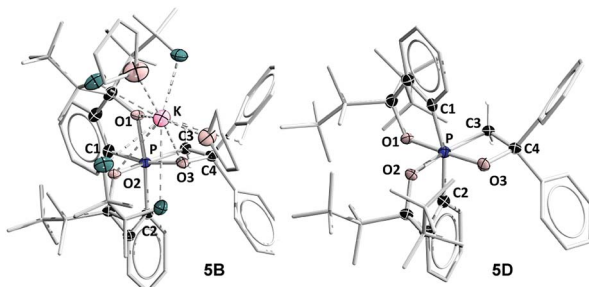


Fig. 2 ORTEP diagram of hexacoordinate oxaphosphates O-fac **5B** and O-mer **5D**³⁸ showing thermal ellipsoids at the 30% probability level. Hydrogen atoms are omitted for clarity. Selected bond lengths (Å) for O-fac **5B**: P–O1, 1.835(2); P–O2, 1.805(2); P–O3, 1.742(2); P–C1, 1.862(4); P–C2, 1.869(3); P–C3, 1.871(3); C3–C4, 1.529(5); O3–C4, 1.450(4). **5D**: P–O1, 1.811(3); P–O2, 1.809(3); P–O3, 1.732(3); P–C1, 1.865(4); P–C2, 1.867(4); P–C3, 1.880(4); C3–C4, 1.539(5); O3–C4, 1.445(5). CCDC: 1856677 for **5B**; 1856676 for **5D**.

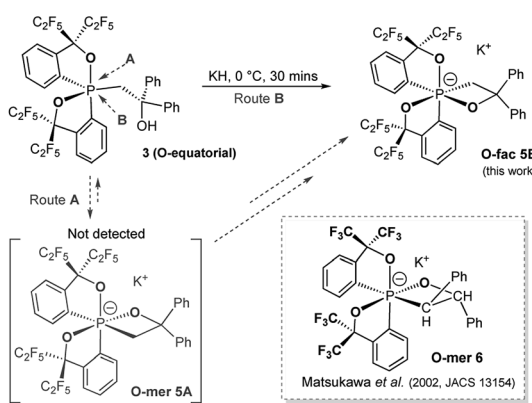
factor responsible for the formation of O-facial geometry.⁵¹ A solid-state structure of **5B** with an independent anion and crown ether-captured cation is shown in Fig. S2.[†]

Compound **5B** represents a rare structural example of an O-facial isomer, despite its predicted thermal stability.^{52,53} The formation of **5B** is in contrast to the previous report by Matsukawa *et al.* using the smaller trifluoromethyl-substituted Martin ligand, from which the O-mer isomer **6** was isolated (Scheme 2 and Table S2[†]). Energetically, the lower lying $\sigma_{P-O(\text{equatorial})}^*$ orbital (in comparison to the $\sigma_{P-C(\text{equatorial})}^*$ orbital) should be more susceptible to the nucleophilic attack (route A) and thus form **5A** as a kinetic product. The reversible reaction and the kinetically less favourable route B would lead to the formation of the thermodynamic product **5B**. However, **5A** was not detected by NMR under our reaction conditions, and thus we could not eliminate the alternative route B. This direct formation of **5B** from **3** through nucleophilic attack at the $\sigma_{P-C(\text{equatorial})}^*$ orbital (route B) may be possible due to the restricted rotation due to the large steric hindrance of the pentafluoroethyl substituents. Indeed, the difference in the chemoselectivity in

deprotonation of **1** between the two ligand systems has been documented.^{47,54} In addition, direct conversion from **5A** to **5B** via other bond cleavage mechanisms or a one step Ray-Dutt twist also have not been probed. Isomerization of hexacoordinate phosphates by non-bond rupture, twist mechanisms has not been investigated experimentally so far. However, those of other hexacoordinate main-group compounds^{55,56} as well as transition metal complexes^{57–59} have been reported plausible based on both experimental and computational studies.⁶⁰

The reaction of the O-apical isomer **4** with KH in THF at room temperature leads to immediate generation of **5C**, detected by $^{31}\text{P}\{\text{H}\}$ NMR spectroscopy as a singlet at -116.9 ppm. This hexacoordinate species then readily isomerizes to **5D** at room temperature, which gives rise to a singlet at -114.9 ppm. An accelerated reaction at 50°C was monitored by $^{31}\text{P}\{\text{H}\}$ NMR (Fig. 3(i and ii)). Furthermore, a differential NOE experiment of **5D** in CD_3CN showed enhancement of different proton signals in the phenyl region when the top and bottom ethylene protons (on C3) were irradiated independently (Fig. S1[†]), implying spatial proximity between the ethylene protons with aryl protons of the two distinct bidentate ligands, thus suggesting an O-mer structure. This has been confirmed by X-ray analysis (Fig. 2 and Table S1[†]). Although single crystals of **5C** could not be obtained for X-ray analysis, we propose an O-meridional structure from a direct nucleophilic attack at a trans position to the equatorial carbon atoms. The corresponding analogue structure, O-mer **7**, was obtained and confirmed by crystallography from the trifluoromethyl substituted Martin ligand system under similar conditions. Although the structure and stereochemistry of this hexacoordinate compound **7** have been discussed in two reports previously,^{27,53} this is the first confirmation by crystallography (Fig. S3 and Table S3[†]). Its synthesis and characterization are described in detail in the ESI.[†]

We can conclude that the final products of deprotonation of the pentacoordinate O-apical isomer **4** and its CF_3^- derivative have different O-mer geometries (**5D** and **7**, respectively). The mechanism of the formation of **5D** remains unclear. If the proposed structure of **5C** is correct, the formation of **5D** may be *via* a one-step Bailar rotation without any bond cleavage.^{55,56} Alternatively, through a bond-rupture pathway, the reaction



Scheme 2 Synthesis of hexacoordinate oxaphosphate O-fac **5B** using a $-\text{C}_2\text{F}_5$ substituted Martin ligand and the structure of Matsukawa's 12-P-6 oxaphosphate O-mer **6**.

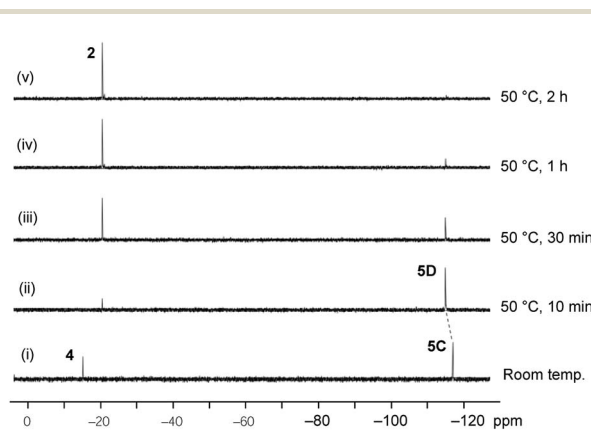
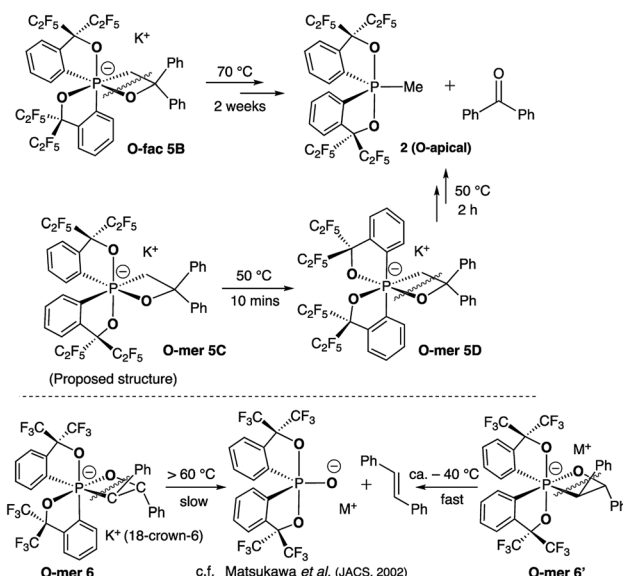


Fig. 3 Time course of the $^{31}\text{P}\{\text{H}\}$ NMR for the conversion of O-mer **5D** and its thermal decomposition at 50°C in THF.

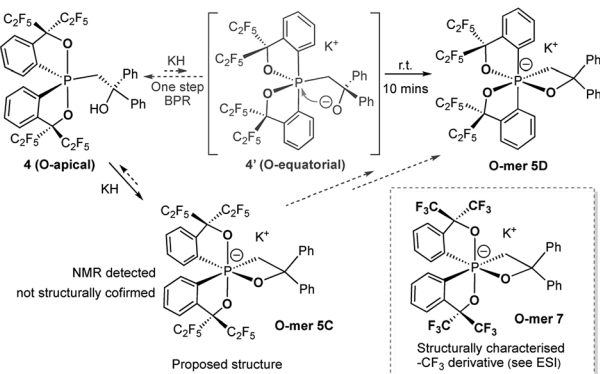


equilibrium may include the unstable O-equatorial intermediate **4'**. Although its concentration in the reaction mixture would be lower than that of **4** due to its higher energy (*ca.* 15 kcal mol⁻¹ higher than **4**),⁶¹ the kinetic barrier for intramolecular nucleophilic attack at the anti-oxygen positions is expected to be much lower, and thus trap **4'** to form the thermodynamic product **5D** (Scheme 3). A similar 10-P-5 O-equatorial intermediate has also been proposed previously by Kawashima *et al.*^{53,62}

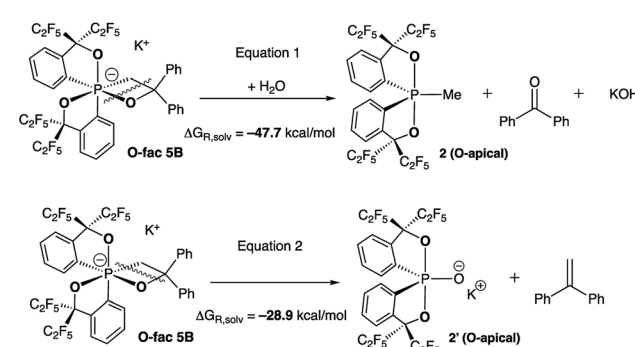
Theoretical calculations at the (SMD:thf)ω-B97XD/def2-tzvpp//ω-B97XD/def2-svp level were carried out to estimate the relative energies of **5A–5D** with and without potassium counter ions (Chart 2). The results show that **5B** and **5D** were lower in energy than their expected kinetic isomers **5A** and **5C**, consistent with the earlier conclusion that they were the thermodynamic products. Although the coordination to potassium cation changes the relative energy gap within both isomeric pairs, the stabilizing effect does not alter the relative energies of the respective pairs, which supports the conclusion that the



Scheme 4 Thermal decomposition of isomers **5B** and **5D**.



Scheme 3 Synthesis of hexacoordinate oxaphosphates **O-mer 5D** in the $-C_2F_5$ system and the structures of 12-P-6 oxaphosphates **5C** and **7**.



Scheme 5 Calculated fragmentation pathways of **O-fac 5B** in the presence and absence of water at the (SMD:thf)ω-B97XD/def2-tzvpp//ω-B97XD/def2-svp level.⁴⁹

coordination to the potassium cation is not the main driving force of isolation of the **O-fac** isomer **5B** (Scheme 4).

At elevated temperatures (70 °C) in solution, the **O-fac** isomer **5B** slowly converts to **2** and benzophenone over 2 weeks. A similar conversion was also observed for **5D** under milder conditions (50 °C) in solution within 2 hours (Fig. 3(ii–v)). Both thermal decomposition leads to cleavage of the P–O bond, which is different to those observed for the CF_3 -substituted **O-mer** isomers **6** and **6'**.²⁷ In the latter case, *trans*-stilbene and hydroxylphosphorane were formed. The difference in the reactivity is likely due to the presence of traces of water.

To verify this, we calculated the energies of fragmentation pathways of the two possible routes from **O-fac 5B** (the lowest-in-energy isomer) to the benzophenone (Scheme 5, eqn (1)) and *trans*-stilbene products (Scheme 5, eqn (2)). The ketone product is much more favoured than the alkene, because of the salt effect of KOH when it is formed in the solution. Investigations to elucidate the different thermal decomposition pathways without water are underway.

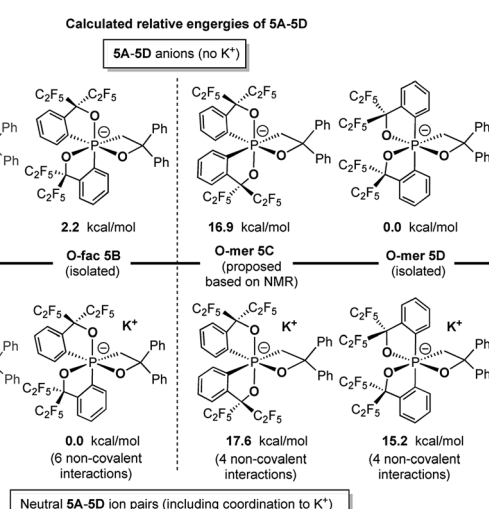


Chart 2 Calculated relative energies of **5A–5D** anions and ion pairs at the (SMD:thf)ω-B97XD/def2-tzvpp//ω-B97XD/def2-svp level.⁴⁹



Conclusions

In conclusion, by using the pentafluoroethyl-substituted derivative of the Martin ligand, the isomeric pair of O-equatorial and O-apical pentacoordinate phosphoranes **3** and **4** was obtained by the reaction of **1** and **2** with *t*BuOK/*n*BuLi and benzophenone. Subsequent deprotonation of **3** and **4** does not yield the expected products **5A** and **5C** based on the kinetically favoured nucleophilic addition pathways, but leads to isolation of the first pair of O-*fac* and O-*mer* hexacoordinate oxaphosphates **5B** and **5D**. Calculations confirmed that **5B** and **5D** are thermodynamic products of their respective isomeric pairs. Their structures were confirmed by X-ray analysis. Although their formation mechanisms remain to be investigated to a full extent, their isolation confirms a strategy to synthesise a hexacoordinate oxaphosphate isomer selectively. The unexpected isolation of the O-*fac* isomer **5B** prompts further experimental and computational studies into both bond-rupture pathways *via* pentacoordinate phosphoranes as well as non-dissociative twist mechanisms. In addition, both the O-*fac* **5B** and the O-*mer* **5D** afforded benzophenone and the methylphosphorane **2** by thermal decomposition. This contrasts with the -CF₃ system, which gave *trans*-stilbene and hydroxylphosphorane, most likely due to the presence of water.

Experimental

All reactions were carried out under N₂ or Ar using standard Schlenk techniques. ¹H NMR (400 MHz), ¹³C NMR (100 MHz), ¹⁹F NMR (376 MHz), and ³¹P NMR (162 MHz) were recorded using a JEOL EX-400 or a JEOL AL-400 spectrometer. ¹H NMR chemical shifts (δ) are given in ppm downfield from Me₄Si, determined by residual chloroform (δ 7.26). ¹⁹F NMR chemical shifts (δ) are given in ppm downfield from external CFCl₃. ³¹P NMR chemical shifts (δ) are given in ppm downfield from external 85% H₃PO₄. The elemental analyses were performed using a Perkin-Elmer 2400 CHN elemental analyzer. Melting points were measured using a Yanaco micro melting point apparatus. Tetrahydrofuran (THF) and diethyl ether (Et₂O) were freshly distilled over CaH₂. Merck silica gel 60 was used for column chromatography.

O-equatorial phosphorane **3**

Under Ar, *n*-BuLi (1.55 M *n*-hexane solution, 0.09 mL, 0.139 mmol) was added to a mixture of phosphorane **1** (47.1 mg, 0.0645 mmol) and *t*-BuOK (1.0 M THF solution, 0.13 mL, 0.13 mmol) suspended with *n*-hexane (5 mL) at 0 °C. The mixture was stirred for 5 min at 0 °C. Benzophenone (48.7 mg, 0.267 mmol) was added at 0 °C. The mixture was then stirred for 4 h at room temperature. The resulting solution was treated with aqueous NH₄Cl at 0 °C and the crude products were extracted with Et₂O (10 mL \times 3). The combined organic layer was dried over MgSO₄ and filtered. After evaporation of the solvent, the residue was purified by TLC (silica gel, *n*-hexane/CH₂Cl₂ = 4/1) to give **3** (18.5 mg, 0.02 mmol, 31%) as white solids. Compound **3** was recrystallized from *n*-hexane/CH₂Cl₂ to yield colourless crystals.

Mp: 135.2–136.0 °C (decomp.); ¹H NMR (CDCl₃): δ = 7.73 (d, ³J_{HH} = 8 Hz, 2H), 7.59 (t, ³J_{HH} = 8 Hz, 2H), 7.37–7.43 (m, 4H), 7.22–7.26 (m, 4H), 7.13–7.19 (m, 6H), 3.84 (d, *J*_{PH} = 16 Hz, 2H), 2.34 ppm (s, 1H); ¹⁹F NMR (CDCl₃): δ = -78.9 (s, 12F), -114.2 (br d, *J*_{FF} = 288 Hz, 2F), -115.5 (br d, *J*_{FF} = 288 Hz, 4F), -115.9 ppm (br d, *J*_{FF} = 288 Hz, 4F); ³¹P NMR (CDCl₃): δ = -2.1 ppm; ¹³C NMR (CDCl₃): δ = 148.0, 133.2, 130.0, 129.9, 128.3, 128.2, 128.0, 126.9, 125.1, 123.1, 75.3, 75.1, 74.8, 53.7, 52.6 ppm. E.A.: calcd (%) for C₃₆H₂₁PF₂₀O₃: C 47.39, H 2.32; found: C 47.35, H 2.06.

O-apical phosphorane **4**

Under Ar, *n*-BuLi (1.63 M *n*-hexane solution, 0.14 mL, 0.228 mmol) was added to a mixture of phosphorane **2** (80.9 mg, 0.110 mmol) and *t*-BuOK (1.0 M THF solution, 0.22 mL, 0.22 mmol) suspended with *n*-hexane (5 mL) at 0 °C. The mixture was stirred for 5 min at 0 °C. Benzophenone (80.7 mg, 0.442 mmol) was added at 0 °C. The mixture was then stirred for 4 h at room temperature. The resulting solution was treated with aqueous NH₄Cl at 0 °C and the crude products were extracted with Et₂O (10 mL \times 3). The combined organic layer was dried over MgSO₄ and filtered. After evaporation of the solvent, the residue was purified by TLC (silica gel, *n*-hexane/CH₂Cl₂ = 4/1) to give **4** (41.8 mg, 0.0458 mmol, 41%) as white solids. Compound **4** was recrystallized from *n*-hexane/CH₂Cl₂ to yield colorless crystals. Mp: 72.0–73.0 °C (decomp.); ¹H NMR (CDCl₃): δ = 8.39 (m, 2H), 7.61–7.69 (m, 6H), 7.30 (dd, ³J_{HH} = 8 Hz, ⁴J_{HH} = 1.5 Hz, 2H), 7.18 (td, ³J_{HH} = 8 Hz, ⁴J_{HH} = 1.5 Hz, 2H), 7.12 (td, ³J_{HH} = 8 Hz, ⁴J_{HH} = 1.5 Hz, 2H), 6.97–7.00 (m, 2H), 6.91–6.95 (m, 2H), 4.32 (s, 1H), 3.59 (dd, *J*_{PH} = 26 Hz, *J*_{HH} = 15 Hz, 1H), 3.55 ppm (dd, *J*_{PH} = 23 Hz, *J*_{HH} = 15 Hz, 1H); ¹⁹F NMR (CDCl₃): δ = -78.3 (s, 6F), -79.2 (t, *J* = 14 Hz, 6F), -114.2 (br d, *J*_{FF} = 290 Hz, 2F), -116.3 (s, 4F), -118.1 ppm (dq, *J*_{FF} = 290 Hz, *J*_{FF} = 14 Hz, 2F); ³¹P NMR (CDCl₃): δ = -15.7 ppm; ¹³C NMR (CDCl₃): δ = 149.1, 146.1, 137.4, 135.1, 134.9, 133.3, 132.7, 131.7, 131.3, 131.1, 128.0, 76.6, 76.0, 51.8, 50.8 ppm. MS(EI(+)): *m/z* = 912 [M]⁺, 913 [M + 1]⁺, 914 [M + 2]⁺, 715 [M-CH₂Ph₂OH].

O-*fac* **5B**

A THF solution of **3** (140 mg, 0.153 mmol) was added to a THF (5 mL) suspension of KH (100 mg, 30% oil dispersion), then the mixture was stirred for 30 min at 0 °C. The supernatant was transferred to a new Schlenk flask. After concentration *in vacuo*, a white solid of **5B** was obtained. **5B** was recrystallized from *n*-hexane/THF to yield colorless crystals (142.5 mg, 0.130 mmol, 85%). Mp: 123.0–124.0 °C (decomp.); ¹H NMR (CDCl₃): δ = 7.87 (dd, *J*_{HH} = 7 Hz, *J*_{PH} = 11 Hz, 1H), 7.31–7.40 (m, 6H), 6.99–7.17 (m, 6H), 6.80–6.98 (m, 5H), 6.60 (dd, *J* = 7 Hz, *J* = 14 Hz, 1H), 4.19 (dd, *J* = 12 Hz, *J* = 30 Hz, 1H), 3.21 (dd, *J* = 12 Hz, *J* = 12 Hz, 1H); ¹⁹F NMR (CDCl₃): δ = -76.7 (s, 3F), -77.4 (s, 3F), -77.9 to -78.3 (m, 6F), -109.1 (d, *J* = 283 Hz, 2F), -109.8 (d, *J* = 283 Hz, 2F), -111.6 to -112.3 (m, 1F), -111.2 to -112.8 (m, 1F), -113.0 to -114.1 (m, 2F); ³¹P NMR (CDCl₃): δ = -107.8 ppm; ¹³C NMR (CDCl₃): δ = 154.0, 153.9, 152.4, 151.7, 151.6, 151.3, 149.5, 133.1, 129.5, 129.0, 128.5, 128.2, 128.0, 127.9, 127.8, 127.7, 127.6, 127.5, 127.3, 127.2, 127.1, 126.6, 126.4, 126.0, 125.8,



125.5, 125.4, 125.3, 124.9, 124.5, 75.8, 65.3 ppm; E.A.: calcd (%) for $C_{48}H_{44}PF_{20}KO_9$ (**5D**·K·18-c-6): C 47.45, H 3.65; found: C 47.86, H 4.29.

O-mer **5D**

A THF solution of **4** (65 mg, 0.071 mmol) and 18-crown-6 (18.7 mg, 0.071 mmol) were added to a suspension of KH (73 mg, 30% oil dispersion), then the mixture was stirred for 30 min at 0 °C. The supernatant was transferred to a new Schlenk flask. After concentration *in vacuo*, a white solid of **5D** was obtained. **5D** was recrystallized from *n*-hexane/THF to yield colorless crystals (10 mg, 0.0074 mmol, 10%). Mp: 131.0–133.0 °C (decomp.); 1H NMR ($CDCl_3$): δ = 7.72 (dd, J_{HH} = 7 Hz, J_{PH} = 14 Hz, 1H), 7.30–7.39 (m, 4H), 7.02–7.17 (m, 4H), 6.92–7.00 (m, 4H), 6.62–6.85 (m, 5H), 3.94 (dd, J = 2 Hz, J = 14 Hz, 1H), 2.54 (ddd, J = 2 Hz, J = 10 Hz, J = 14 Hz, 1H); ^{19}F NMR ($CDCl_3$): δ = -76.5 (q, J = 8 Hz, 3F), -77.0 (q, J = 8 Hz, 3F), -78.0 (m, 6F), -104.2 (d, J = 286 Hz, 1F), -107.9 (d, J = 290 Hz, 1F), -110.4 (d, J = 286 Hz, 1F), -111.2 to -112.8 (m, 3F), -113.0 to -114.1 (m, 3F); ^{31}P NMR ($CDCl_3$): δ = -118.1 ppm; ^{13}C NMR ($CDCl_3$): δ = 156.1, 154.3, 153.9, 153.8, 154.1, 153.5, 152.3, 130.0, 128.6, 128.4, 128.1, 127.7, 127.6, 126.8, 126.2, 126.1, 125.6, 125.5, 125.4, 124.6, 75.0, 55.5 ppm. E.A.: calcd (%) for $C_{56}H_{60}PF_{20}KO_{11}$ (**5B**·K·18-c-6·2THF): C 49.49, H 4.45; found: C 48.98, H 4.48.

Thermal conversion of **3** to **4**

A solution of compound **3** (11.8 mg, 0.0129 mmol) in benzene (1.0 mL) was heated at 80 °C for 8 h. After concentration *in vacuo*, compound **4** was obtained (11.2 mg, 0.0123 mmol, 98%) as a white solid. The spectral data were consistent with those of the product obtained in the synthesis of **4**.

Reaction of **3** with KH to give benzophenone by heating

A THF (1 mL) solution of **3** (13.8 mg, 0.0151 mmol) was added to a THF (0.5 mL) suspension of KH (excess), then the mixture was stirred for 10 min at 0 °C. Then, the mixture was heated for two weeks at 70 °C. The mixture was extracted with Et_2O (2 × 40 mL), and the organic layer was washed with brine (2 × 30 mL) and dried over anhydrous $MgSO_4$. After filtering the organic layer through SiO_2 and removing the solvents by evaporation, the residue was separated by reversed-phase HPLC (CH_3CN) to afford **2** (RT = 41.6 min: 10.4 mg, 0.0142 mmol, 94%) as a white solid and benzophenone (RT = 19.7 min: 0.0261 mg, 0.0143 mmol, 95%) as a white solid. Benzophenone: 1H NMR ($CDCl_3$): δ = 7.81 (d, J_{HH} = 8.0 Hz, 4H), 7.59 (t, J_{HH} = 8.0 Hz, 2H), 7.48 ppm (t, J_{HH} = 8.0 Hz, 4H). The data of **2** are consistent with that in the reported paper.³⁷

Reaction of **4** with KH to give benzophenone by heating

A THF (0.5 mL) solution of **4** (28.2 mg, 0.0309 mmol) was added to a THF (0.3 mL) suspension of KH (excess), then the mixture was stirred for 10 min at 0 °C. The solution was transferred to an NMR tube under N_2 , and the mixture was heated for 2 hours at 50 °C. The NMR spectra were recorded. The mixture was

extracted with Et_2O (2 × 40 mL), and the organic layer was washed with brine (2 × 30 mL) and dried over anhydrous $MgSO_4$. After filtering the organic layer through SiO_2 and removing the solvents by evaporation, the residue was separated by reversed-phase HPLC (CH_3CN) to afford **2** (RT = 41.2 min: 22.1 mg, 0.0302 mmol, 98%) as a white solid and benzophenone (RT = 19.2 min: 5.4 mg, 0.0296 mmol, 96%) as a white solid. Benzophenone: 1H NMR ($CDCl_3$): δ = 7.81 (d, J_{HH} = 8.0 Hz, 4H), 7.59 (t, J_{HH} = 8.0 Hz, 2H), 7.48 ppm (t, J_{HH} = 8.0 Hz, 4H). The data of **2** are consistent with that in the reported paper.³⁷

Conflicts of interest

There are no conflicts to declare.

Acknowledgements

This work was supported by the NNSFC (21542004), Young and middle-aged scientific and technological innovation talents of Shenyang Science and Technology Bureau (RC170140), the Liaoning Province Natural Science Foundation (20170540721), Basic research on the application of Industrial Development of Shenyang Science and Technology Bureau (18013027), the Distinguished Professor Project of Liaoning province, and the JSPS KAKENHI Grant (24109002) from the Ministry of Education, Culture, Sports, Science and Technology, Japan. We also thank the Chinese Scholarship Council (20183058).

Notes and references

- 1 N. V. Timosheva, A. Chandrasekaran and R. R. Holmes, *Inorg. Chem.*, 2006, **45**, 10836–10848.
- 2 R. R. Holmes, *Acc. Chem. Res.*, 2004, **37**, 746–753.
- 3 S. D. Lahiri, G. Zhang, D. Dunaway-Mariano and K. N. Allen, *Science*, 2003, **299**, 2067–2071.
- 4 R. R. Holmes, *Pentacoordinated Phosphorus: Structure and Spectroscopy*, American Chemical Society, 1980.
- 5 B. E. Maryanoff and A. B. Reitz, *Chem. Rev.*, 1989, **89**, 863–927.
- 6 G. Wittig and M. Rieber, *Liebigs Ann.*, 1949, **562**, 187–192.
- 7 S. Matsukawa, K. Kajiyama, S. Kojima, S.-Y. Furuta, Y. Yamamoto and K.-Y. Akiba, *Angew. Chem., Int. Ed.*, 2002, **41**, 4718–4722.
- 8 S. Kumaraswamy, C. Muthiah and K. C. K. Swamy, *J. Am. Chem. Soc.*, 2000, **122**, 964–965.
- 9 J. A. Deiters, R. R. Holmes and J. M. Holmes, *J. Am. Chem. Soc.*, 1988, **110**, 7672–7681.
- 10 P. Wang, Y. Zhang, R. Glaser, A. Streitwieser and P. v. R. Schleyer, *J. Comput. Chem.*, 1993, **14**, 522–529.
- 11 K. Kajiyama, M. Yoshimune, M. Nakamoto, S. Matsukawa, S. Kojima and K.-Y. Akiba, *Org. Lett.*, 2001, **3**, 1873–1875.
- 12 R. S. Berry, *J. Chem. Phys.*, 1960, **32**, 933–938.
- 13 I. Ugi, D. Marquarding, H. Klusacek, P. Gillespie and F. Ramirez, *Acc. Chem. Res.*, 1971, **4**, 288–296.
- 14 P. Gillespie, P. Hoffman, H. Klusacek, D. Marquarding, S. Pfohl, F. Ramirez, E. A. Tsolis and I. Ugi, *Angew. Chem., Int. Ed. Engl.*, 1971, **10**, 687–715.



15 S. Matsukawa, H. Yamamichi, Y. Yamamoto and K. Ando, *J. Am. Chem. Soc.*, 2009, **131**, 3418–3419.

16 A. J. Arduengo, C. A. Stewart, F. Davidson, D. A. Dixon, J. Y. Becker, S. A. Culley and M. B. Mizen, *J. Am. Chem. Soc.*, 1987, **109**, 627–647.

17 A. Brand and W. Uhl, *Chem.-Eur. J.*, 2019, **25**, 1391–1404.

18 C. B. Caputo, L. J. Hounjet, R. Dobrovetsky and D. W. Stephan, *Science*, 2013, **341**, 1374–1377.

19 D. W. Stephan, *Angew. Chem., Int. Ed.*, 2017, **56**, 5984–5992.

20 D. Hellwinkel, *Chem. Ber.*, 1966, **99**, 3642–3659.

21 D. Hellwinkel, *Chem. Ber.*, 1966, **99**, 3628–3641.

22 D. Hellwinkel, *Angew. Chem., Int. Ed. Engl.*, 1965, **4**, 356.

23 D. Hellwinkel, *Chem. Ber.*, 1965, **98**, 576–587.

24 J. Lacour and D. Linder, *Chem. Rec.*, 2007, **7**, 275–285.

25 J. Lacour, C. Ginglinger, C. Grivet and G. Bernardinelli, *Angew. Chem., Int. Ed. Engl.*, 1997, **36**, 608–610.

26 T. A. Engesser, M. R. Lichtenthaler, M. Schleep and I. Krossing, *Chem. Soc. Rev.*, 2016, **45**, 789–899.

27 For an example of an asymmetric catalysis by a hexacoordinate chiral phosphate species see Ooi and coworkers' work: D. Uraguchi, H. Sasaki, Y. Kimura, T. Ito and T. Ooi, *J. Am. Chem. Soc.*, 2018, **140**, 2765–2768.

28 S. Matsukawa, S. Kojima, K. Kajiyama, Y. Yamamoto, K.-y. Akiba, S. Re and S. Nagase, *J. Am. Chem. Soc.*, 2002, **124**, 13154–13170.

29 M. Nakamoto and K.-y. Akiba, *J. Am. Chem. Soc.*, 1999, **121**, 6958–6959.

30 N. V. Timosheva, A. Chandrasekaran, R. O. Day and R. R. Holmes, *J. Am. Chem. Soc.*, 2002, **124**, 7035–7040.

31 K. V. P. P. Kumar, N. S. Kumar and K. C. K. Swamy, *New J. Chem.*, 2006, **30**, 717–728.

32 C. Martin, *Science*, 1983, **221**, 509–514.

33 J. C. Martin and E. F. Perozzi, *Science*, 1976, **191**, 154–159.

34 E. F. Perozzi and J. C. Martin, *J. Am. Chem. Soc.*, 1979, **101**, 1591–1593.

35 F. Medici, G. Gontard, E. Derat, G. Lemiere and L. Fensterbank, *Organometallics*, 2018, **37**, 517–520.

36 H. Lenormand, J.-P. Goddard and L. Fensterbank, *Org. Lett.*, 2013, **15**, 748–751.

37 X.-D. Jiang, K.-i. Kakuda, S. Matsukawa, H. Yamamichi, S. Kojima and Y. Yamamoto, *Chem.-Asian J.*, 2007, **2**, 314–323.

38 I. Richter, M. Penka and R. Tacke, *Inorg. Chem.*, 2002, **41**, 3950–3955.

39 I. Serrano, X. Sala, E. Plantalech, M. Rodriguez, I. Romero, S. Jansat, M. Gomez, T. Parella, H. Stoeckli-Evans, X. Solans, M. Font-Bardia, B. Vidjayacoumar and A. Llobet, *Inorg. Chem.*, 2007, **46**, 5381–5389.

40 F. Julia, D. Bautista, J. M. Fernandez-Hernandez and P. Gonzalez-Herrero, *Chem. Sci.*, 2014, **5**, 1875–1880.

41 C. Zhan, Z. Han, B. O. Patrick and D. P. Gates, *Dalton Trans.*, 2018, **47**, 12118–12129.

42 K. C. K. Swamy and N. S. Kumar, *Acc. Chem. Res.*, 2006, **39**, 324–333.

43 J. Kobayashi, K. Goto, T. Kawashima, M. W. Schmidt and S. Nagase, *J. Am. Chem. Soc.*, 2002, **124**, 3703–3712.

44 X.-D. Jiang, S. Matsukawa, S. Kojima and Y. Yamamoto, *Inorg. Chem.*, 2012, **51**, 10996–11006.

45 X.-D. Jiang, S. Matsukawa, K.-i. Kakuda, Y. Fukuzaki, W.-L. Zhao, L.-S. Li, H.-B. Shen, S. Kojima and Y. Yamamoto, *Dalton Trans.*, 2010, **39**, 9823–9829.

46 X.-D. Jiang, S. Matsukawa, H. Yamamichi and Y. Yamamoto, *Inorg. Chem.*, 2007, **46**, 5480–5482.

47 X.-D. Jiang, S. Matsukawa, H. Yamamichi and Y. Yamamoto, *Heterocycles*, 2007, **73**, 805–824.

48 K. Kajiyama, M. Yoshimune, S. Kojima and K.-y. Akiba, *Eur. J. Org. Chem.*, 2006, 2739–2746.

49 For computational details, please see ESI.†

50 Due to the minimal collection strategy, the data set provided a reasonable solution for structural confirmation. However, bonding parameters are not reliable for discussion.

51 The addition of crown ether before, after or at the same time of the deprotonating reagent did not affect the reaction results.

52 R. S. Michalak, S. R. Wilson and J. C. Martin, *J. Am. Chem. Soc.*, 1984, **106**, 7529–7539.

53 T. Kawashima, K. Watanabe and R. Okazaki, *Tetrahedron Lett.*, 1997, **38**, 551–554.

54 K.-y. Akiba, S. Matsukawa, K. Kajiyama, M. Nakamoto, S. Kojima and Y. Yamamoto, *Heterroat. Chem.*, 2002, **13**, 390–396.

55 H. S. Rzepa and M. E. Cass, *Inorg. Chem.*, 2007, **46**, 8024–8031.

56 M. Amati and F. Lelj, *Theor. Chem. Acc.*, 2008, **120**, 447–457.

57 J. G. Gordon and R. H. Holm, *J. Am. Chem. Soc.*, 1970, **92**, 5319–5332.

58 N. A. P. Kane-Maguire, T. W. Hanks, D. G. Jurs, R. M. Tollison, A. L. Heatherington, L. M. Ritzenthaler, L. M. McNulty and H. M. Wilson, *Inorg. Chem.*, 1995, **34**, 1121–1124.

59 R. A. Palmer, R. C. Fay and T. S. Piper, *Inorg. Chem.*, 1964, **3**, 875–881.

60 S. Alvarez, *Chem. Rev.*, 2015, **115**, 13447–13483.

61 S. Kojima, K. Kajiyama, M. Nakamoto and K.-y. Akiba, *J. Am. Chem. Soc.*, 1996, **118**, 12866–12867.

62 H. Miyake, N. Kano and T. Kawashima, *Inorg. Chem.*, 2011, **50**, 9083–9098.

